Anisotropic etching of polymer films by high energy (~100s of eV) oxygen atom neutral beams

Siddhartha Panda and Demetre J. Economou[a)]
Plasma Processing Laboratory, Department of Chemical Engineering, University of Houston, Houston, Texas 77204-4792

Lee Chen
Chen Laboratories, Austin, Texas 78758

(Received 21 April 2000; accepted 4 December 2000)

An inductively coupled high density plasma source was used to generate an energetic (100s of eV), high flux (equivalent of ~10s mA/cm^2) oxygen atom neutral beam. Positive ions were extracted from the plasma and neutralized by a metal grid with high aspect ratio holes. High rate (up to 0.6 μm/min), microloading-free, high aspect ratio (up to 5:1) etching of polymer with straight sidewalls of sub-0.25 μm features was demonstrated. The polymer etch rate increased with power and showed a shallow maximum with plasma gas pressure. The etch rate increased roughly as the square root of the boundary voltage (which controls neutral beam energy), and was independent of substrate temperature. The latter observation suggests that spontaneous etching did not occur. The degree of neutralization of the extracted ions was estimated to be greater than 99% at the base case conditions used in this work. © *2001 American Vacuum Society.* [DOI: 10.1116/1.1344909]

I. INTRODUCTION

Charging damage as a result of plasma processing is a serious issue in device fabrication including damage to thin gate oxides,[1] notching,[2,3] sidewall bowing, and aspect ratio dependent etching (ARDE).[4] These artifacts may be caused by differential charging of microstructures arising from the difference in angular distributions of electrons and ions. Ions are highly anisotropic while electrons are not. As more electrons initially impact the sidewalls of a feature, the sidewalls charge negatively with respect to the bottom surface. Charging can distort the trajectory of further incoming ions[5–8] resulting in etching of the sidewalls (bowing) or of the foot of the polysilicon gate (notching). In ARDE, the etch rate of features normally decreases as the feature aspect ratio increases. Distortion of ion trajectories, due to local electric fields formed by charging of the sidewalls, may result in an ion flux to the sidewalls at the expense of that in the trench bottom in deep trenches. This depletion of the flux to the trench bottom may contribute to a reduction of the vertical etch rate. Another problem of distorted wall profile associated with surface charging is dovetailing.[7]

Plasma induced charging damage becomes more critical as device dimensions continue to shrink and aspect ratios keep increasing. One way to minimize or avoid charging damage is by using neutral beams instead of a plasma. However, for neutral beam technology to be a viable alternative, the neutral beam energy and flux needs to be comparable to those obtained during reactive ion etching.

Several studies using neutral beams have been reported in the literature. Mizutani and Yunogami[9] developed a neutral beam etcher using a Kaufman-type ion source to generate Ar ions in the 200–700 eV range. Charge exchange with the background neutral gas produced the energetic neutral beam. A CHF_3 microwave plasma independently provided neutral (thermalized) radicals to assist the etching process. The etch rate of SiO_2 with the neutral beam was about 10 nm/min at 700 eV and this was half of the etch rate obtained with a comparable ion beam. Capacitance–voltage ($C-V$) measurements showed that there was no reduction in breakdown voltage (compared to a standard) when the samples were subjected to neutral beam etching. In contrast, breakdown occurred at lower voltages when the samples were subjected to ion beam etching. To overcome the limitation of low etch rates, a coaxial neutral beam assisted etcher was developed.[10] In this configuration, a coaxial discharge tube generated two cylindrical plasmas; the inner one served as the neutral beam source and the outer one served as the neutral radical source. A 500 eV Ar neutral beam gave a maximum etch rate of 60 nm/min for SiO_2. To overcome the limitation of lack of etch uniformity obtained with the coaxial etcher, a tandem neutral beam etcher was further developed,[11] where the neutral beam source and the neutral radical source were arranged in tandem. Highly anisotropic and uniform etching was obtained, but the maximum SiO_2 etch rate was only 76 nm/min.

Using the charge exchange mechanism, a low energy (10–20 eV) neutral stream of chlorine atoms was extracted from an electron cyclotron resonance (ECR) plasma.[12,13] An etch rate of 100 Å/min for Si was obtained which was about 10% of that realized with ion stream etching. Goeckner, Bennett, and Cohen[14] produced hyperthermal neutrals by accelerating ions to a surface where they were neutralized and reflected. Using an O_2/Ar mixture, they obtained resist etch rates up to 22 nm/min and a flux of about 2×10^{14} $1/cm^2/s$. Shimokawa and co-workers[15] used an ion source to develop a fast-atom beam. The beam energy was 1–3 keV and the beam current was 0.1–1 mA/cm^2, with about 95% neutralization. Resist etch rates of 0.3–0.5 μm/min with high selectivity (GaAs:resist = 30:1) were obtained. Damage to the

[a)]Electronic mail: economou@uh.edu

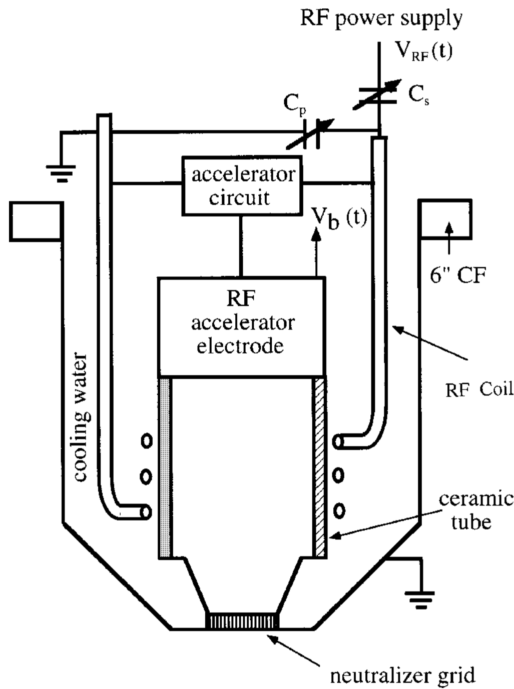

FIG. 1. Schematic of the neutral beam source.

wafers was low. However, micro-loading and sidewall bowing were observed. Chen and Yang,[16] used a grid to extract positive ions out of an inductively coupled plasma source. A second grid was used to neutralize these ions before interacting with a wafer downstream. They realized high rate anisotropic etching of polymer films.

Neutral beams with much lower (<10 eV) energy have also been reported. Giapis, Moore, and Minton,[17] using a laser detonation technique, obtained a F-atom beam with a flux of 2×10^{14} atoms/cm^2/s and energy less than 10 eV. The ion fraction was less than 1%. An etch rate of 300 Å/min for Si with 14% undercutting was obtained. Campos *et al.*[18] used laser vaporization of a cryogenic Cl_2 film to generate a hyperthermal (maximum energy 6 eV) molecular beam. The etch rate of Si with the energetic beam was greater than that with thermal chlorine by a factor >30. Using a hyperthermal beam (~1 eV) of molecular chlorine produced by free jet expansion of a Cl_2 gas heated in a graphite furnace, Suzuki, Hiraiska, and Nishimatsu[19] obtained highly anisotropic etching of poly-Si with an etch rate of 3.1 nm/min. Selectivity over SiO_2 was more than 1000. $C-V$ studies showed that the damage levels were much lower than those by plasma or ion beam processes. Using the same technique to produce hyperthermal Cl_2, Ono *et al.*[20] etched GaAs at 1.5 μm/min.

In this study, an energetic neutral beam of oxygen atoms was generated and used to etch polymer films. In contrast to Chen and Yang,[16] a single extraction/neutralization grid was used greatly simplifying the system.

II. EXPERIMENT

A schematic of the neutral beam source used in this work is shown in Fig. 1. An inductively coupled plasma is generated in the cylindrical ceramic (alumina) tube of 2.7 cm inside diameter and 8.4 cm length. Radio frequency power at 13.56 MHz (OEM-6, ENI Power Systems) is supplied through a matching network to a rf coil. The ceramic tube and the rf coil are immersed in de-ionized cooling water. The water temperature is controlled by a chiller (Model 2095, Forma Scientific). For the experiments reported here, the water temperature is fixed at 18 °C. A tunable accelerator circuit (including a tuning capacitor) taps a fraction of the power from the rf power supply to the rf accelerator electrode to generate a boundary voltage (V_b) that accelerates ions out of the plasma. The boundary voltage provides control of the ion energy and hence the neutral beam energy. The extracted ions pass through a neutralizer grid where they are neutralized. The rf grounded aluminum grid is 1 in. in diameter. The transparency of the grid is 38% with cylindrical holes 0.007 in. in diameter and 0.042 in. in height.

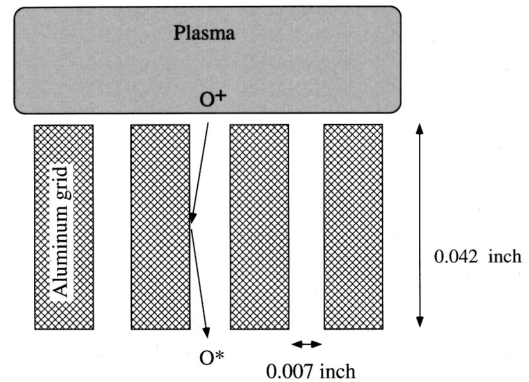

FIG. 2. Schematic of the near-gird region.

Figure 2 gives a schematic of the near-grid region. Neutralization can occur due to charge exchange collisions of the ions with the background neutrals or by surface neutralization on the grid. For plasma chamber pressures lower than 50 mTorr, the ion mean free path is larger than the sum of the sheath thickness and the gridhole length (grid thickness). Thus charge exchange is not expected to be a major contributor to the neutralization process. Neutralization is thought to occur by the grazing angle collision of ions with the grid surface. Ions coming out of the plasma have an angular spread of several degrees off normal. The periodically collapsing sheath over the grid holes causes a fraction of the ions to enter the holes with even larger angles off normal.

Figure 3 shows a schematic of the experimental setup. The neutral beam source is placed on the top flange of a 6 in. six way cross (MDC). Pressure in the plasma chamber is measured by a Baratron (MKS) with a readout unit (MKS) and the boundary voltage is charted on a digitizing oscilloscope (11401, Tektronix). Ultrahigh purity O_2 feed gas (Iweco, Houston, TX) is fed through a leak valve. The water cooled substrate holder, a 3.75 in. diameter hollow S.S. plate, is mounted on a 10 in. linear motion feedthrough (Huntington). The substrate water temperature is regulated by a chiller (Tempryte-HS-3500, Bay Voltex). Double sided carbon

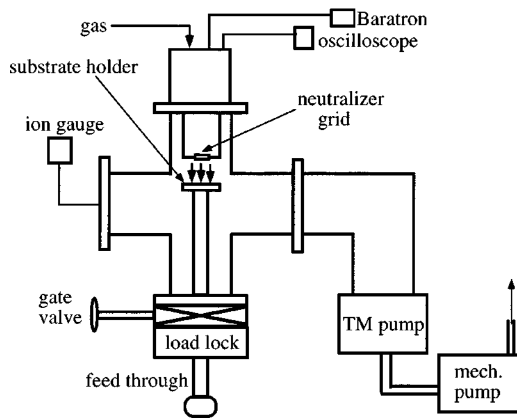

FIG. 3. Schematic of the experimental setup.

tapes (Electron Microscopy Sciences, Fort Washington, PA) are used to ensure good thermal contact of the sample with the substrate electrode. The downstream chamber is evacuated by a turbo-molecular pump (Turbovac 360 V, Leybold) backed by a mechanical pump (Trivac D25BCS, Leybold). An ion gauge (0572-K7360-301, Varian) is used to measure the base pressure and the pressure at the downstream region with an ion gauge controller (Model 290, MKS). A stainless steel shutter can be moved over the sample to control the exposure time of the sample to the beam. A laser interferometry system (5 mW He–Ne laser at 632.8 nm, 3222H-PC, Hughes Aircraft Corp.) is used for *in situ* measurement of the etch rate of blanket films. Etch rates were also verified by profilometry.

Surface composition of sample films was determined using x-ray photoelectron spectroscopy (XPS), using an aluminum x-ray source at 15 keV. Samples after etching were stored under dry nitrogen and were transferred quickly to the XPS chamber. Patterned wafers were analyzed by scanning electron microscopy (SEM).

III. RESULTS AND DISCUSSION

Due to the high power density used in the source, a high degree of molecular oxygen dissociation is expected (O atom concentration greater than ten times the O_2 molecule concentration), as predicted by a discharge model.[21] Thus, the dominant positive ions in the plasma and (consequently) the dominant energetic neutral species in the bean are expected to be O^+ and O, respectively. The degree of positive ion neutralization was estimated as follows: The ion density in the plasma (in the $10^{11}/cm^3$ range) was estimated from the ion saturation current measured by a Langmuir probe immersed in the plasma. The electron temperature (few eV) was estimated by a computer simulation procedure as described in Ref. 21. Knowing the ion density and the electron temperature, a Bohm flux of positive ions was calculated (the plasma is essentially electropositive due to the high degree of dissociation of molecular oxygen). The expected ion flux entering the grid holes was calculated from the Bohm flux and the grid transparency (38%). A planar probe placed 1 in. downstream of the grid was then used to measure the ion current exiting the grid. The ratio of the downstream measured positive ion current to the ion current entering the holes of the grid was taken as the degree of neutralization. Using this procedure, the degree of neutralization was found to be >99% for the base case conditions used in this work (Table I).

TABLE I. Range of parameter values and base case conditions used for experimental work.

Parameters	Range	Base case
Power (W)	300–700	500
Plasma pressure (mTorr)	10–50	20
Boundary voltage, V_b(V)	70–160	100
Substrate temperature, T_s(°C)	5–85	20
Grid-substrate distance, d (cm)	3.5–13.5	3.5
Beam-substrate angle (degrees)	0–87.5	0

A. Blanket resist

Samples of 1.1-μm-thick *i*-line resist on silicon were etched and various experimental parameters were varied to study their effect. The base case conditions used are shown in Table I, where V_b is the boundary voltage, T_s is the temperature of the substrate holder, and d is the grid-to-wafer distance. While studying the effect of a parameter, the rest are kept at the base case values unless mentioned otherwise. Error bars on the data points in the figures below represent the repeatability of the data from sample to sample.

1. Effect of power

Figure 4 shows the effect of input rf power on etch rate. The rf power controls the ion density in the plasma and consequently the neutral beam flux. The etch rate increases with power from 0.20 μm/min at 300 W to 0.42 μm/min at 700 W. The etch rate behavior at high powers indicates that the ion density and hence the neutral flux is approaching a saturation value with power. This saturation behavior was also seen in the O-atom emission followed by optical emission spectroscopy.[22] Similar results were obtained for the etch rate of photoresist in an ECR system by Pang *et al.*,[23,24] although their system is different than ours, in the sense that our wafer is not immersed in the plasma. When the boundary voltage V_b was left free to attain its natural value (i.e., not

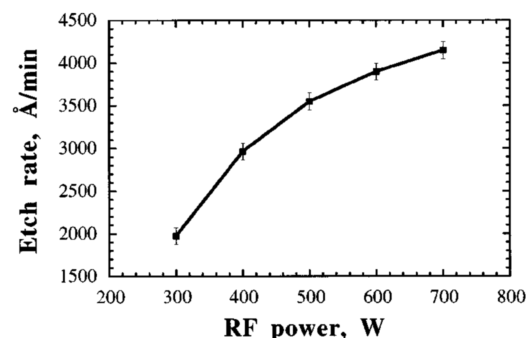

FIG. 4. Effect of rf power on etch rate (with V_b adjusted to its base case value). Other conditions at the base values (see Table I).

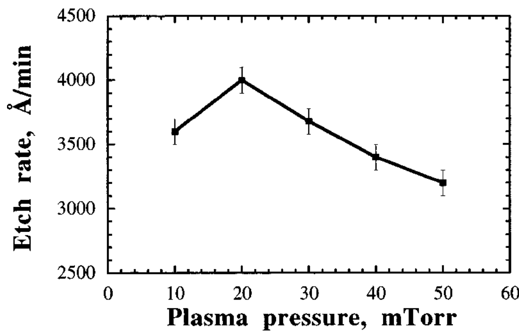

FIG. 5. Effect of plasma gas pressure on etch rate. Other conditions at the base values (see Table I).

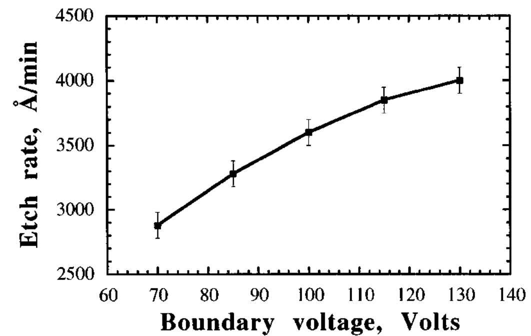

FIG. 6. Effect of boundary voltage (related to beam energy) on etch rate. Other conditions at the base values (see Table I).

adjusted to the base case value when power was changed), a linear behavior of etch rate with power was obtained, whereby the etch rate increased from 0.20 μm/min at 300 W (with a V_b of 100 V) to 0.60 μm/min at 700 W (with a V_b of 150 V). An increase of etch rate with power was also seen by Chen and Yang.[16]

2. Effect of pressure

The effect of pressure in the plasma region on etch rate is shown in Fig. 5. For the conditions used, a maximum of 0.4 μm/min is seen at 20 mTorr, increasing from 0.36 μm/min at 10 mTorr and decreasing to 0.32 μm/min at 50 mTorr. This is probably a manifestation of the behavior of the ion density in the plasma. The measured ion density in the bulk plasma was found to have a shallow maximum with pressure in the 10–50 mTorr range. At lower pressures, the ion density is lower as the gas density is lower. At higher pressures, the electron temperature decreases[25] which causes lower Bohm velocities reducing the ion flux. More importantly, ion density gradients (from the bulk to the surface) become steeper as pressure increases, further reducing the ion flux to surfaces in contact with the plasma. The behavior of ion flux and thus neutral beam flux with pressure is manifested in the behavior of the etch rate. A maximum in polymer etch rate with pressure in oxygen plasmas has been observed by Munoz and Dominguez,[26] Juan and Pang,[24] Hartney *et al.*[27] and Hsiao, Miller, and Kellock.[28] It should be noted, however that, in contrast to our case, in all these studies the sample was immersed in the plasma. Therefore, thermalized oxygen radicals and molecules are expected to play a significant role in these works.

3. Effect of boundary voltage (V_b)

The boundary voltage is a measure of the effective plasma potential. As such it is also a measure of the energy of ions exiting the plasma. Hence the boundary voltage directly affects the neutral beam energy. The etch rate increases with increasing boundary voltage, from 0.29 μm/min at 70 V to 0.4 μm/min at 130 V, as shown in Fig. 6. The etch rate scales approximately with the square root of the boundary voltage. Similar behavior for polymer in-plasma etch rate versus bias voltage (which is a measure of the ion energy) was observed by Jurgensen, Hutton, and Taylor[29] in a helicon oxygen plasma. Assuming that the expression proposed by Steinbruchel[30] (where the etch yield is proportional to the square root of the ion energy at high ion energies) is valid, it can be hypothesized that the neutral beam energy is directly proportional to V_b.

4. Effect of distance from neutralizer grid (d)

The effect of sample distance from the neutralizer grid is shown in Fig. 7(a). The distance was varied using a linear motion feedthrough. The etch rate decreased as the distance between the wafer and the grid was increased, from 0.4 μm/min at 3.5 cm to 0.06 μm/min at 13.5 cm. This is probably due to the divergence of the beam. The behavior of the etch rate is not proportional to the inverse of the square of the distance from the source ($1/r^2$ dependence) as observed by Krech[31] for etching polymers with an oxygen atom beam. As

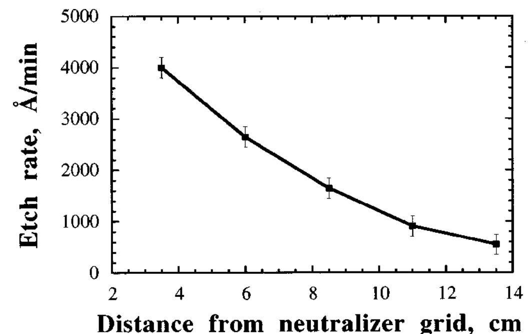

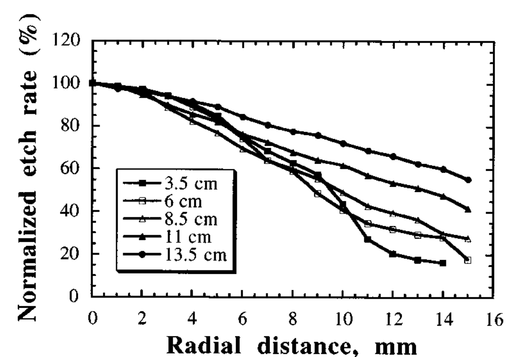

FIG. 7. (a) Effect of the distance of wafer from the neutralizer grid on etch rate. Other conditions at the base values (see Table I). (b) Effect on etch uniformity of wafer to neutralizer grid distance. Other conditions at the base values (see Table I).

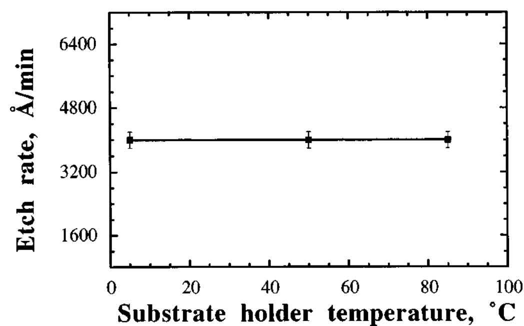

FIG. 8. Effect of substrate holder temperature on etch rate. Other conditions at the base values (see Table I).

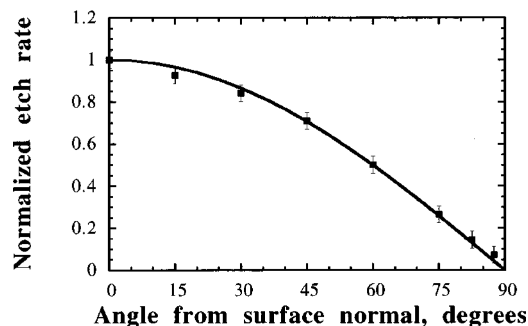

FIG. 9. Effect of beam incidence angle on etch rate. Other conditions at the base values (see Table I).

seen from Fig. 7(a), the etch rate is higher than expected from the $1/r^2$ dependence (being about $1/r^{1.44}$). A similar result was obtained by Giapis, Moore, and Minton[17] with their hyperthermal F-atom neutral beam etching of Si. They attributed this to a nonlinear flux dependence and/or high ambient (thermalized) F-atom pressure at the wafer region. In our case, the pressure at the wafer region is rather low ($\sim 10^{-4}$ Torr) and hence the presence of thermalized radicals cannot be a contributing factor. This is corroborated by the lack of dependence of the etch rate on substrate temperature (see Fig. 8). Decreasing etch rates with increasing wafer to source distance have also been observed in other systems. Pang, Sung, and Ko[23] found an almost linear decrease in etch rate of resist in an oxygen ECR system. This was attributed to the decrease with distance of ion density which, along with neutrals, contributed to etching. The uniformity of etching is shown in Fig. 7(b). Better uniformity is obtained at longer distances. Thus, the distance brings about a trade-off between etch rate and uniformity. Pang and co-workers[23] also obtained better uniformity as the wafer to source distance was increased.

5. Effect of substrate holder temperature (T_s)

For the temperature range used, the etch rate is independent of the wafer temperature as seen from Fig. 8. The thermalized neutral gas density at the wafer is rather low due to low pressures in the downstream (wafer) region ($\sim 10^{-4}$ Torr). This indicates that etching occurs by the energetic beam, not by thermalized species. This has the important implication, as will be seen later, that undercutting is not a problem in our system.

6. Effect of beam incidence angle

The etch rate as a function of the angle between the sample surface normal and the beam is shown in Fig. 9. It is seen that the experimental values (symbols) follow a cosine curve (solid line). Gokan, Itoh, and Esho[32] studied the effect of oxygen ion beam angle dependence on the etch rate of different polymers [poly(methylmethacrylate), polyimide and AZ1350J] in reactive ion beam etching (RIBE). The etch rate decreased with angle but did not follow a cosine profile. Physical sputtering of Si and metals[33] gives a maximum in the etch rate with angle (normally in the range 40°–60°). Chang *et al.*[34] found that the maximum etch yield of Si with Ar^+, with $Cl/Ar^+=600$, was at normal incidence and the yield started decreasing at 30°–40° off-normal angles. They argued that the chemical reactivity of the adsorbed chlorine atoms compensated for the less efficient ion momentum transfer at off-normal incidence. Okano and Horiike[35] studied the angular dependence of the etch rate of Si with (i) Ar^+, (ii) Ar^+ plus Cl^+, and (iii) Ar^+ with an independent effusive source of Cl_2. Subtracting the etch rate profile of case (iii) from that of case (i) gave a profile which followed a cosine curve. This indicated that chemically assisted etching followed a cosine curve. The results of Fig. 9 indicate that in our system, physical sputtering does not play a role.

7. Effect of beam energy on film composition

High energy (≥ 1 keV) Ar ion bombardment has been found to cause polymer degradation.[36] Similar effects were observed in etching of polymers in N_2O[37] and SF_6[38] plasmas at ion energies of about 150 eV. Volatilization of oxygen, nitrogen and hydrogen, aided by the impact of energetic ions, was found to leave graphitized carbon in the polymer surface layers. The resulting loss of the dielectric insulator property can be an important issue. Joubert *et al.*[38] found polymer degradation in oxygen plasmas when the ion energy was too high, and this was attributed to sputtering being favored over chemical etching at higher energies.

The surface composition of the polymer films used in this work was investigated using XPS to study the effect of bombardment by energetic O-atom neutral beams. As spontaneous etching is not expected in our system, XPS analysis can be expected to give information on the beam-surface interaction. The hydrogen content cannot be measured by XPS and the nitrogen and argon contents were found to be negligible. Only carbon and oxygen peaks were observed in the XPS spectra. The carbon content of a nominally unetched film (it was etched for 10 s to remove any surface adsorbed species), corresponding to a value of the boundary voltage V_b of 0 V, was 73.2%. This increased to 75.2% at $V_b=70$ V and 77.5% at $V_b=100$ V and $V_b=125$ V, indicating that for the energies used, graphitization is not a serious problem. Importantly, aluminum was not detected in the film, indicating that contamination from sputtering of the aluminum neutralization grid was not an issue.

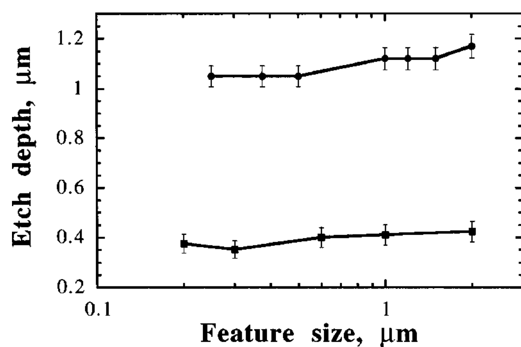

FIG. 10. Effect of feature size on etch depth for two samples. Each sample contained features with width from 0.2–2 μm. Other conditions at the base values (see Table I).

B. Patterned resist

A SiO_2 mask with feature sizes between 2 and 0.2 μm on a 1.2-μm-thick *i*-line resist coated over silicon was used to study neutral beam etching of patterned films.

1. ARDE

Figure 10 shows the etch depth as a function of feature size for two samples etched to different depths, one being about 0.4 μm and the other being about 1.05 μm. The etch time for all feature sizes was the same within each of the two samples. In both cases the variation in etch depth is within 6% of the reported value, indicating negligible ARDE. Figure 11 shows a SEM of a patterned wafer with a 0.35 μm feature. On the left side of the line there is an open field while on the right side are more (nested) features. The identical etch depths on both sides of the line again show lack of ARDE. ARDE has been observed in etching of polymers in oxygen plasmas.[29] Charging of sidewall features may be one of the factors responsible for ARDE[5–8] in reactive ion etching (RIE) systems. A neutral beam mitigates any charging problems. The angular distribution of the energetic ions has been identified as another possible cause for ARDE.[4]

2. Anisotropy

Charging of sidewall features can result in distortion of the wall profile leading to notching, bowing, dovetailing, etc.

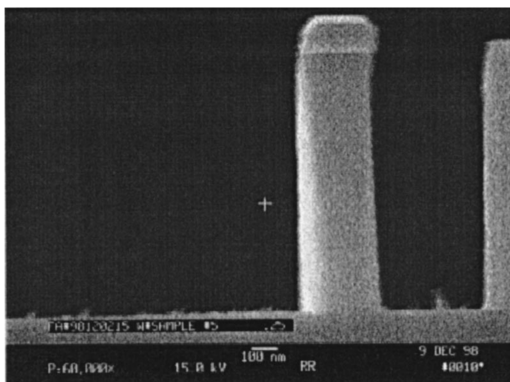

FIG. 11. SEM of an etched 0.35 μm feature. White marker size is 0.1 μm.

As seen from Fig. 11, etching with a neutral beam results in a high degree of anisotropy without any wall profile distortion. Another factor contributing to wall profile distortion is lateral etching by thermalized neutrals causing mask undercut. Unlike in traditional plasma etching systems, in our system the pressure at the wafer region is about two orders of magnitude lower than that in the plasma region. Hence the density of the thermalized neutrals is low, minimizing lateral etching. Anisotropy in RIE and RIBE of polymers with oxygen has been found to increase with ion energy.[23,29,32,37] In our work, the beam energy, while sufficient to obtain a high etch rate, was not too high to result in reflection and scattering causing bowing, as was seen by Shimokawa *et al.*[15] In plasma etching, lower pressures bring about higher anisotropy as there are fewer collisions in the sheath and ions arrive at the surface with smaller angular spread. In addition, lower pressures result in lower etchant densities. This may restrict the range of pressures used. In our system, for pressures <50 mtorr, the diameter and aspect ratio of the holes of the grid, rather than pressure, control the collimation of the beam.

IV. CONCLUSIONS

An inductively coupled plasma was used to generate a high energy (100s of eV) oxygen atom neutral beam. Neutralization of the ions extracted from the plasma was accomplished by grazing angle surface collision with a high aspect ratio aluminum grid. The etching performance of the source was investigated. Blanket *i*-line resist was etched and the effect of different parameters studied. Etch rates up to 0.6 μm/min were obtained. The etch rate increased with the input rf power which controlled the beam flux. A square root dependence of the etch rate on the boundary voltage, which is a measure of the beam energy, was observed. The etch rate showed a shallow maximum at about 20 mTorr plasma pressure. The wafer temperature did not have an effect on the etch rate indicating that etching was due to the beam alone and not due to thermalized neutrals. The etch rate decreased with distance from the source but did not follow as strong as a $1/r^2$ dependence. The behavior of the etch rate with the beam angle followed a cosine curve. XPS analysis indicated that graphitization of the polymer was not a problem for the beam energies used. Also, Al could not be detected on the etched wafers by XPS, indicating that sputtering of the grid was not occurring. Patterned wafers with feature sizes 0.2–2 μm were etched. For the aspect ratios used ($\sim$5), there was hardly any aspect ratio dependence on etch rate. A high degree of anisotropy in etched features was obtained and there was no undercut. The degree of neutralization of the extracted ions was estimated to be greater than 99% at the base case conditions used in this work (Table I).

ACKNOWLEDGMENTS

Work at the University of Houston was supported by the State of Texas through the Texas Advanced Technology Program and the National Science Foundation (CTS-9713262).

[1]C. T. Gabriel and J. P. McVittie, Solid State Technol. **35**, 81 (1992).
[2]S. Samukawa, Appl. Phys. Lett. **64**, 3398 (1994).
[3]N. Fujiwara, T. Maruyama, and M. Yoneda, Jpn. J. Appl. Phys., Part 1 **35**, 2450 (1996).
[4]R. A. Gottscho, C. W. Jurgensen, and D. J. Vitkavage, J. Vac. Sci. Technol. B **10**, 2133 (1992).
[5]G. S. Hwang and K. P. Giapis, J. Appl. Phys. **82**, 566 (1997).
[6]S. G. Ingram, J. Appl. Phys. **68**, 500 (1990).
[7]J. C. Arnold and H. H. Sawin, J. Appl. Phys. **70**, 5314 (1991).
[8]D. J. Economou and R. Alkire, J. Electrochem. Soc. **135**, 941 (1988).
[9]T. Mizutani and T. Yunogami, Jpn. J. Appl. Phys., Part 1 **29**, 2220 (1990).
[10]T. Yunogami, K. Yogokawa, and T. Mizutani, J. Vac. Sci. Technol. A **13**, 952 (1995).
[11]K. Yokogawa, T. Yunigami, and T. Mizutani, Jpn. J. Appl. Phys., Part 1 **35**, 1901 (1996).
[12]T. Tsuchizawa, Y. Jin, and S. Matsuo, Jpn. J. Appl. Phys., Part 1 **33**, 2200 (1994).
[13]Y. Jin, T. Tsuchizawa, and S. Matsuo, Jpn. J. Appl. Phys., Part 2 **34**, L465 (1995).
[14]M. J. Goeckner, T. K. Bennett, and S. A. Cohen, Appl. Phys. Lett. **71**, 980 (1997).
[15]F. Shimokawa, H. Tanaka, Y. Uenishi, and R. Sawada, J. Appl. Phys. **66**, 2613 (1989); F. Shimokawa, J. Vac. Sci. Technol. A **10**, 1352 (1992).
[16]L. Chen and Q. Yang, The Electrochemical Society Proceedings, edited by G. S. Mathad and M. Meyyappan, 1996, Vol. 96-12, p. 332.
[17]K. P. Giapis, T. A. Moore, and T. K. Minton, J. Vac. Sci. Technol. A **13**, 959 (1995).
[18]F. X. Campos, G. C. Weaver, C. J. Waltman, and S. R. Leone, J. Vac. Sci. Technol. B **10**, 2217 (1992).
[19]K. Suzuki, S. Hiraoka, and S. Nishimatsu, J. Appl. Phys. **64**, 3697 (1988).
[20]T. Ono, H. Kashima, S. Hiraoka, K. Suzuki, and A. Jahnke, J. Vac. Sci. Technol. B **9**, 2798 (1991).
[21]S. Panda, D. J. Economou, and M. Meyyappan, J. Appl. Phys. **87**, 8323 (2000).
[22]S. Panda, D. J. Economou, and L. Chen (unpublished).
[23]S. W. Pang, K. T. Sung, and K. K. Ko, J. Vac. Sci. Technol. B **10**, 1118 (1992).
[24]W. H. Juan and S. W. Pang, J. Vac. Sci. Technol. B **12**, 422 (1994).
[25]J. Forster and W. Holber, J. Vac. Sci. Technol. A **7**, 899 (1989).
[26]J. Munoz and C. Dominguez, J. Vac. Sci. Technol. B **13**, 2179 (1995).
[27]M. A. Hartney, W. M. Greene, D. S. Soane, and D. W. Hess, J. Vac. Sci. Technol. B **6**, 1892 (1988).
[28]R. Hsiao, D. Miller, and A. Kellock, J. Vac. Sci. Technol. A **14**, 1028 (1996).
[29]C. W. Jurgensen, R. S. Hutton, and G. N. Taylor, J. Vac. Sci. Technol. B **10**, 2542 (1992).
[30]C. Steinbruchel, Appl. Phys. Lett. **55**, 1960 (1989).
[31]R. H. Krech, NASA Final Report, Prepared under Contract No. NAS3-25968 by Physical Sciences, Inc., Andover, MA, March 1993.
[32]H. Gokan, M. Itoh, and S. Esho, J. Vac. Sci. Technol. B **2**, 34 (1984).
[33]B. Chapman, *Glow Discharge Processes* (Wiley, New York, 1980).
[34]J. P. Chang, J. C. Arnold, G. C. H. Zhau, H.-S. Shin, and H. H. Sawin, J. Vac. Sci. Technol. A **15**, 1853 (1997).
[35]H. Okano and Y. Horiike, Jpn. J. Appl. Phys., Part 1 **20**, 2429 (1981).
[36]B. J. Bachman and M. J. Vasile, J. Vac. Sci. Technol. A **7**, 2709 (1989).
[37]O. Joubert, J. Pelletier, and Y. Arnal, J. Appl. Phys. **65**, 5096 (1989).
[38]O. Joubert, J. Pelletier, C. Fiori, and T. A. N. Tan, J. Appl. Phys. **67**, 4291 (1990).